trpm7 Regulation of *in Vivo* Cation Homeostasis and Kidney Function Involves Stanniocalcin 1 and *fgf23*

Michael R. Elizondo, Erine H. Budi, and David M. Parichy

Department of Biology (M.R.E., D.M.P.) and Graduate Program in Molecular and Cellular Biology (E.H.B.), University of Washington, Seattle Washington 98195; and Graduate Program in Molecular and Cell Biology (M.R.E.), University of Texas, Austin, Texas 78712

The transient receptor potential melastatin 7 (trpm7) channel kinase is a primary regulator of magnesium homeostasis *in vitro*. Here we show that trpm7 is an important regulator of cation homeostasis as well as kidney function *in vivo*. Using zebrafish *trpm7* mutants, we show that early larvae exhibit reduced levels of both total magnesium and total calcium. Accompanying these deficits, we show that *trpm7* mutants express higher levels of stanniocalcin 1 (*stc1*), a potent regulator of calcium homeostasis. Using transgenic overexpression and morpholino oligonucleotide knockdown, we demonstrate that *stc1* modulates both calcium and magnesium levels in *trpm7* mutants and in the wild type and that levels of these cations are restored to normal in *trpm7* mutants when stc1 activity is blocked. Consistent with defects in both calcium and phosphate homeostasis, we further show that *trpm7* mutants develop kidney stones by early larval stages and exhibit increased levels of the anti-hyperphosphatemic factor, fibroblast growth factor 23 (*fgf23*). Finally, we demonstrate that elevated *fgf23* expression contributes to kidney stone formation by morpholino knockdown of *fgf23* in *trpm7* mutants. Together, these analyses reveal roles for *trpm7* in regulating cation homeostasis and kidney function *in vivo* and implicate both *stc1* and *fgf23* in these processes. **(*Endocrinology* 151: 5700–5709, 2010)**

The two closely related genes, *TRPM7* and *TRPM6*, encode transient receptor potential (TRP) family proteins that function as divalent cation channels with C-terminal α-kinase domains that regulate channel activity (1–5). TRP melastatin 7 (Trpm7) and Trpm6 are preferentially permeable to a number of divalent cations (6–11), including magnesium and calcium, and studies of these channels have provided new insights into magnesium and calcium homeostasis (1, 9–15). Trpm7 and Trpm6 function as either homomeric channels or as heteromeric channels with one another (1, 10, 16–19). Whereas Trpm7 channels are expressed across a wide range of tissues (1, 19, 20), Trpm6 channels have a somewhat more limited distribution, being found primarily in organs that regulate physiological ion levels, such as the kidney and intestines (7, 20–22). Mammalian Trpm7 also functions in sensing extracellular calcium and magnesium in neurons (23–25) and in regulating cell adhesion (26, 27), whereas human mutations in *TRPM6* are linked to hypomagnesemia with secondary hypocalcemia (14, 28).

Numerous studies have shown the importance of Trpm7 for cation homeostasis *in vitro*, yet the early lethality of Trpm7 mutations in mammals has precluded analyzing roles in whole-organism cation homeostasis (29). By contrast, zebrafish *trpm7* mutants survive into embryonic and postembryonic stages, permitting analyses of developmental and physiological *trpm7* functions *in vivo* (30). Zebrafish *trpm7* mRNA is detectable in all adult tissues (Elizondo, M. R., and D. M. Parichy, unpublished data) and is expressed widely in embryos and larvae, with particularly high transcript abundance in the tubules of the pronephric and mesonephric kidneys, and in the corpuscles of Stannius (CS), a teleost-specific gland that regulates physiological ion homeostasis (30–32). As em-

ISSN Print 0013-7227 ISSN Online 1945-7170
Printed in U.S.A.

doi: 10.1210/en.2010-0853 Received July 27, 2010. Accepted August 25, 2010.
First Published Online September 29, 2010

Abbreviations: CaSR, Calcium-sensing receptor; CS, corpuscles of Stannius; dpf, days post fertilization; hpf, hours post-fertilization; EGFP, enhanced green fluorescent protein; FGF23, fibroblast growth factor 23; hpf, hours post fertilization; IRES, internal ribosome entry site; qPCR, quantitative RT-PCR; stc1, stanniocalcin 1; TRP, transient receptor potential; Trpm7, TRP melastatin 7.

bryos, *trpm7* mutants have defects in the survival of melanized pigment cells, melanophores, and also develop a transient unresponsiveness to touch (33–35). As larvae, these mutants exhibit severe defects in growth and skeletogenesis while also developing kidney stones (30). The known functions of mammalian Trpm7 channels suggest the pleiotropic phenotypes of zebrafish *trpm7* mutants may be related to altered cation homeostasis and kidney function.

Here we show that zebrafish *trpm7* mutants exhibit multiple defects in physiological homeostasis. We find that *trpm7* mutants have reduced levels of whole-embryo total calcium and total magnesium by 3 and 4 d post fertilization (dpf), respectively, and we demonstrate that the CS-specific gene, stanniocalcin 1 (*stc1*) is a downstream mediator of altered cation levels in *trpm7* mutants. Additionally, we show that *trpm7* mutants develop kidney stones by 5 dpf and express elevated levels of the anti-hyophosphatemic factor *fgf23*, whereas morpholino knockdown of fgf23 reduces the incidence of kidney stones in the mutant background. Together, our findings provide important new information about *trpm7* functions and lay the groundwork for further studies of its *in vivo* roles in cation and phosphate homeostasis as well as kidney function.

Materials and Methods

Strains and rearing conditions

Fish were reared at 28.5 C (except as noted below) with a 14-h light, 10-h dark cycle. Mutants were *trpm7*^{j124e1}, *trpm7*^{j124e2}, and *trpm7*^{b508}, with most experiments using the latter allele.

Total calcium and magnesium assays

For each sample tested, 25 embryos or larvae were pooled, anesthetized with MS222, rinsed briefly in nanopure H_2O, and collected in a 1.5-ml microcentrifuge tube. Fish were then dried at 65 C for 30–45 min, at which time 125 μl 1 M HCl was added to each tube and acid denatured overnight at 95 C with occasional tapping or brief centrifugation to collect solution at the bottom of the tube. Tubes were then centrifuged at maximum speed for 15 min, and supernatant was collected. To assess total calcium and magnesium content from the supernatant, we used QuantiChrom calcium and magnesium assays (BioAssay Systems, Hayward CA; DICA-500 and DIMG-250). Although *trpm7* mutants exhibit growth retardation at later larval stages, sizes of embryos and early larvae are indistinguishable from wild type (30, 35).

For magnesium assays, the manufacturer's protocol was used with half-reactions and 5 μl of each sample tested for 2- to 5-dpf fish. Absorbances were read at 490 nm before and after addition of 10 μl EDTA to obtain blank readings for individual wells. Statistical analyses were performed using JMP version 8.0.1 for Macintosh (SAS Institute, Cary, NC).

Total RNA isolation and cDNA synthesis

For RNA preparations, 10 embryos were pooled, anesthetized in MS222, and homogenized in 200 μl TRIzol (Invitrogen, Carlsbad, CA). RNA preps were performed as specified in the manufacturer's protocol, resuspended in 13 μl H_2O, and quantitated using a NanoDrop 1000 spectrophotometer (ThermoScientific, Wilmington, DE). Superscript III and RNase Inhibitor (Invitrogen) were used in cDNA synthesis reactions primed with oligo dT primers, as per manufacturer's protocol. cDNAs were diluted with 100 μl TE before use.

Quantitative RT-PCR (qPCR)

For qPCR, 50-μl reactions were performed in triplicate using 0.5 μl AmpliTaq (Applied Biosystems, Foster City, CA), 5 μl GeneAmp 10× PCR buffer, 1 μl 12.5× SYBR Green (Sigma-Aldrich, St. Louis, MO), 1 μl 10 mM dNTPs, 2 μl 2.5 μM forward and reverse primer mix, and 1.5 μl diluted cDNA. For cycling, a Chromo4 real-time instrument (MJ Research, Waltham, MA) was used with the following program: an initial denaturing step of 94 C for 3 min followed by 40 cycles of 94 C for 20 sec, 56 C for 20 sec, 72 C for 20 sec and a final elongation step of 72 C for 5 min. For each primer set, no-template control reactions were performed. Before qPCR, multiple primer sets were tested for amplification efficiency, amplification without primer-dimer formation, and optimal annealing temperature using gradient PCR with annealing temperatures ranging from 54–62 C. Selected primers were determined to have optimal amplification efficiency at 56 C annealing without formation of primer-dimers. Primer sets (forward, reverse, 5′ to 3′) used for quantitative qPCR were: β-actin, GCATCACACCTTCTACAACGAG, AGAGTCCATCACGATACCAGTG; *stc1* (endogenous), GCAGGGCAGGAGTATTTATTAGTG, CAGAAAACATCTCAACCACATCCAG; and *stc1* (transgenic), TCACCTGTTCGCCAGAAACG, CCAAAAGACGGCAATATGGTGG. Primers used for molecular cloning (attB1F and attB1R sites *underlined*): *stc1*, (<u>GGGGACAAGTTTGTACAAAAAAGCAGGCTACC</u>ATGCTCCTGAAAGCGGATTTC, <u>GGGGACCACTTTGTACAAGAAAGCTGGGT</u>TTAAGGACTTCCCACGATGGAGC).

qPCR data were collected using Chromo4 Opticon Monitor 3 software. For relative expression analysis between *trpm7* mutants and wild-type siblings, data were analyzed using REST 2008 software (36). For absolute expression analysis of transgene induction after heat shock, data were analyzed using Qgene software (37). All data presented are representative of three biological replicates.

In situ hybridization

Gene expression analyses by *in situ* hybridization followed standard methods (38) using Sp6-synthesized digoxigenin riboprobes targeted to 753 bp of *stc1* (NM_200539) and 758 bp of *fgf23* (AY753222) cDNAs. Wild-type and mutant embryos were stained for identical times, and *in situ* hybridizations were replicated on three different occasions using embryos from multiple clutches ($n > 300$ total embryos examined). Typical expression patterns are shown, although mutants could sometimes show defects of greater or lesser severity.

Transgenic expression constructs

To construct an *stc1*-expressing transgenic line, we used the Tol2kit (39) and Multisite Gateway reagents (Invitrogen). We amplified a full-length *stc1* cDNA with primers containing *att*B

flanking sequences, inserted the amplicon into pDONR221 and verified integrity of the open reading frame by sequencing. We used the pDONR-*stc1* clone as the middle entry vector, combined with p5E-*hsp70 5′* entry vector, p3E-IRES-EGFPpA 3′ entry vector, and the pDestTol2pA2 destination vector from the Tol2kit. The resulting vector comprised an expression cassette with a heat-shock protein *hsp70* promoter controlling expression of the full-length *stc1* followed by enhanced green fluorescent protein (EGFP) linked by an internal ribosome entry site (IRES). We coinjected this hsp70::stc1-IRES-EGFP plasmid with Tol2 mRNA transcribed from the pCS2FA-transposase plasmid (40). Injected embryos were heat shocked at 38.5 C for 30 min at 24 h post fertilization (hpf) and then screened for mosaic expression of EGFP at 4 h after heat shock. GFP-positive embryos were reared to adulthood and screened for germline integration through their progeny. Identified germline carriers were used to establish stable transgenic lines and the strongest GFP-expressing line was used for experiments; we did not observe significant inter-embryo variation in the ubiquitous pattern of *hsp70*-induced expression as assayed by EGFP fluorescence. Similar results were observed in other transgenic lines.

Heat-shock induction

Two methods were used for heat-shock induction experiments. To screen transgenic progeny for GFP, a single heat shock was performed by placing embryos in 250-ml glass culture dishes (Carolina Biological, Burlington, NC) and then placing dishes in a shaking water bath set to 38.5 C and heat shocking embryos for 20 min. For repeated heat shocking over a period of several days, embryos were placed in clear plastic cups with mesh-covered holes to provide circulating water flow. Cups were then placed in a 10-gallon acrylic aquarium with a drain and 28.5 C flowing fish system water. Temperature was controlled using a ProcessTech heater and temperature controller (Aquatic Ecosystems, Apopka, FL). The heater controller was then plugged into an electrical timer set for a cycle for 30 min on, 5.5 h off.

Antisense morpholino oligonucleotide injections

Morpholinos to *stc1* (stc1-MO: GAAATCCGCTTTCAGGAGCATGTC) and *fgf23* (fgf23-sb1: GCAACAGGTAGGCTACTCACTGTAT) were designed by GeneTools LLC (Philomath, OR). stc1-MO targets the translational start site, whereas fgf23-sb1 targets the exon1/intron1 splice donor site. Disrupted splicing of fgf23 pre-mRNA by fgf23-sb1 was verified by RT-PCR (41) (data not shown). Lyophilized morpholino was resuspended in 300 μl 1× Danieau buffer. Concentrations were determined by diluting 2 μl in 20 μl 0.1 M HCl, measuring the absorbance at 265 nm using a NanoDrop (ThermoScientific) spectrophotometer and calculating the concentration as recommended by the manufacturer. Morpholinos were then diluted to 0.2 mM in 1× Danieau buffer, and 4.8–6.4 ng stc1-MO and 6.5 ng fgf23-sb1 were injected into wild-type embryos at the one- to two-cell stage.

Detection of kidney stones

We used a 0.5% (wt/vol) solution of alizarin red (Sigma-Aldrich) diluted in nanopure H_2O and adjusted to pH 7.5 with sodium bicarbonate. For staining, we incubated embryos or larvae in petri dishes in a final concentration of 0.004% alizarin red diluted in 10% Hank's solution (42). After overnight incubation, fish were briefly washed in 10% Hank's before anesthetizing with MS222 and imaging under epifluorescence illumination using a Texas Red filter set. To assess kidney stone migration, individual fish were imaged immediately after a brief rinse and then allowed to recover in 10% Hank's for 12 h, when they were imaged for a second time.

Results

Reduced total calcium and magnesium in *trpm7* mutants

In humans, mutations in *TRPM6* lead to hypomagnesemia because of decreased Mg^{2+} reabsorption by the kidney and intestines, which in turn disrupts calcium homeostasis in the parathyroid gland, resulting in hypocalcemia (14, 28). Because Trpm6 channels are thought to act in heteromeric complexes with Trpm7 to regulate Mg^{2+} homeostasis (16, 19), defects arising from *TRPM7* mutations might be expected to overlap with those exhibited by *TRPM6* mutants. We therefore tested whether disruptions to cation homeostasis in zebrafish *trpm7* mutants are similar to those arising from mammalian Trpm6 mutation. Because we could not extract sufficient serum from zebrafish embryos, we examined physiological cation levels as a proxy, by comparing the total calcium and magnesium contents of wild-type and mutant embryos from 2–5 dpf.

For total calcium, mutants did not differ significantly from wild type at 2 dpf but exhibited significantly reduced levels by 3 dpf and still more pronounced reductions at 4–5 dpf (Fig. 1A). For total magnesium, we found reduced levels in mutants at 4 and 5 dpf (Fig. 1B). Although not a direct measurement of serum cation levels, the reduced

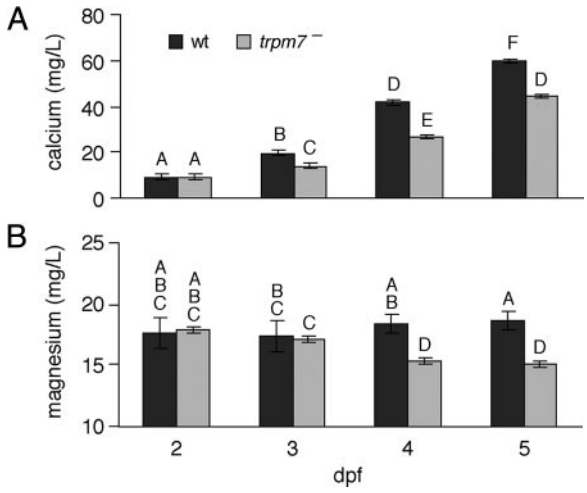

FIG. 1. Total calcium and magnesium concentrations in *trpm7* mutants. A and B, Calcium (A) and magnesium (B) levels are shown as least squares means ± SE after controlling for batch-specific variation (n = 120 mutant and wild-type samples at stages 2–5 dpf). By overall ANOVA, calcium $F_{(7,112)} = 467$ ($P < 0.0001$) and magnesium $F_{(7,112)} = 33.8$ ($P < 0.0001$). Samples with the *same letters* are not significantly different by Tukey-Kramer honestly significant difference test ($\alpha = 0.05$). wt, Wild type.

total cation levels are consistent with hypocalcemia and hypomagnesemia in mutants.

Altered stanniocalcin-mediated regulation of divalent cation homeostasis in *trpm7* mutants

Terrestrial animals obtain calcium only from their diet and are typically challenged by hypocalcemic conditions. The primary regulators of calcium homeostasis, PTH and PTHrP, are, therefore, anti-hypocalcemic factors (43–45). In contrast, fish are surrounded by an abundant external supply of calcium and can be challenged with preventing hypercalcemia, which they accomplish by controlling ion influx through the gills, kidneys, and intestine. The teleost-specific CS regulates the rates of ion influx at these sites by secreting anti-hypercalcemic stanniocalcins (46–49) (reviewed in Ref. 50). Zebrafish stanniocalcin 1 (*stc1*) is expressed exclusively by the CS of embryos and early larvae (Fig. 2, A and B), although it is expressed more broadly in adults (31, 51). Because *trpm7* is expressed particularly strongly in the CS as well (30, 31), we asked whether *trpm7*-dependent changes in calcium levels might be associated with changes in *stc1* regulation.

To test this, we assayed *stc1* expression in *trpm7* mutant embryos by qPCR. We found significant increases in *stc1* transcript abundance in *trpm7* mutants compared with wild type beginning at 2 dpf and extending at least through 5 dpf (Fig. 2C). The increased *stc1* expression in mutants preceded the detectable deficiency in total calcium (Fig. 1A), suggesting that up-regulated *stc1* and its anti-hypercalcemic activity may be directly responsible for reduced total calcium in *trpm7* mutants.

stc1 overexpression reduces total calcium as well as total magnesium

trpm7 mutants exhibited up-regulated *stc1* expression followed by decreased total calcium and total magnesium (Figs. 1 and 2C). Although decreased calcium is explicable

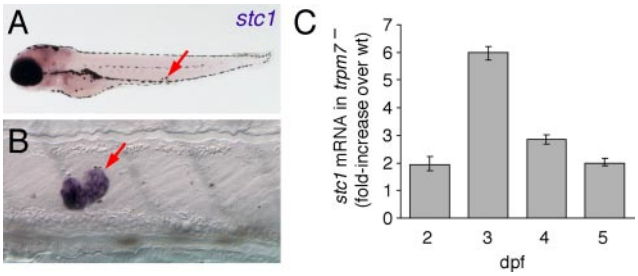

FIG. 2. Expression of *stc1* and increased transcript abundance in *trpm7* mutants compared with wild type (wt). A, Low-magnification view showing expression in CS (*arrow*). *Purple* coloration in head is background due to probe trapping. B, Higher magnification of CS. C, qPCR showing that *stc1* mRNA is more abundant in *trpm7* mutants at each stage examined. Values were normalized to β-actin and scaled relative to wild-type sibling levels of *stc1*. *Error bars* represent 95% confidence intervals; all $P < 0.05$ compared with wild-type levels.

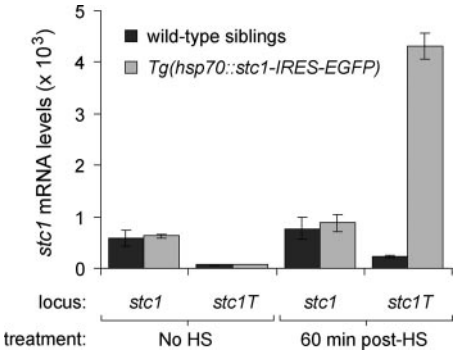

FIG. 3. Induction of transgenic *stc1* with and without heat shock (HS) assayed by qPCR. Both endogenous transcript (*stc1*) and transgene-derived transcript (*stc1T*) are assayed. Induction of the transgene is observed in *Tg*(*hsp70*::*stc1-IRES-EGFP*) embryos 60 min after heat shock of 5-dpf larvae (means ± SE). Absolute expression levels were scaled to those for β-actin. Endogenous *stc1* levels were assayed with primers targeting the 3′-untranslated region, whereas transgenic *stc1* were assayed with primers targeting the 3′-coding sequence and the IRES sequence of the transgene. *stc1T* transcript levels in wild-type sibling larvae and transgenic larvae without heat shock are comparable to those observed with no-template qPCR controls (data not shown).

by the anti-hypercalcemic activity of stc1, we hypothesized that stc1 also might negatively regulate magnesium levels. To test this idea in a wild-type background, we generated a heat-shock-inducible transgenic line to overexpress stc1, *Tg*(*hsp70*::*stc1-IRES-EGFP*). After 38.5 C heat shock for 30 min, we confirmed transgene-specific expression of *stc1* (*stc1T*) by qPCR (Fig. 3).

To mimic the increased *stc1* expression of *trpm7* mutants in a wild-type genetic background, we heat shocked transgenic and nontransgenic sibling embryos for 30 min at 6-h intervals between 40 and 120 hpf. After heat shock, we sorted embryos for the presence or absence of the transgene by GFP fluorescence, and we performed ion assays as described above. We found that heat-shocked *Tg*(*hsp70*::*stc1-IRES-EGFP*) embryos exhibited reduced total calcium and total magnesium compared with heat-shocked, nontransgenic siblings (Fig. 4). This confirmed the anti-hypercalcemic activity of stc1 and supported the hypothesis that stc1 influences magnesium homeostasis, either directly or indirectly.

Inhibition of *stc1* in *trpm7* mutants restores total calcium and total magnesium levels

Inhibition of zebrafish *stc1* activity increased calcium levels (51). Additionally, our results from overexpressing *stc1* in wild-type embryos suggested that, in *trpm7* mutants, decreased total calcium and total magnesium may result from *stc1* up-regulation. We therefore tested whether normal total calcium and total magnesium levels could be restored in a *trpm7* mutant background simply by inhibiting *stc1* translation by morpholino oligonucleotide injection.

Embryos injected with a morpholino targeted to *stc1* (stc1-MO) were morphologically indistinguishable from

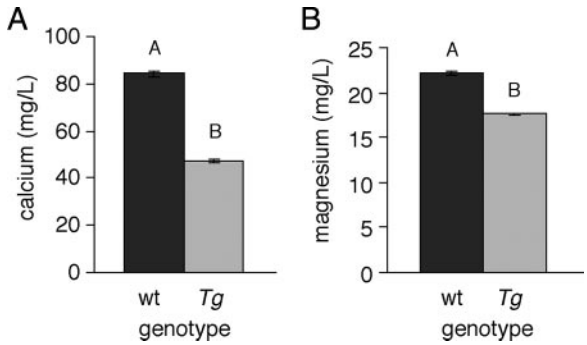

FIG. 4. Total calcium and magnesium levels in *Tg*(*hsp70::stc1-IRES-EGFP*) larvae compared with wild-type siblings. A and B, Reduced total calcium (A) and total magnesium (B) levels in heat-shocked transgenic (*Tg*) larvae compared with heat-shocked nontransgenic [wild type (wt)] siblings. Calcium and magnesium levels represent least squares means ± SE after controlling for variation among batches (n = 16 mutant and wild-type samples at 5 dpf). By overall ANOVA, calcium $F_{(1,14)} = 499$ ($P < 0.0001$) and magnesium $F_{(1,14)} = 313$ ($P < 0.0001$). Samples with different letters in each panel are significantly different by Tukey-Kramer honestly significant difference test ($\alpha = 0.05$).

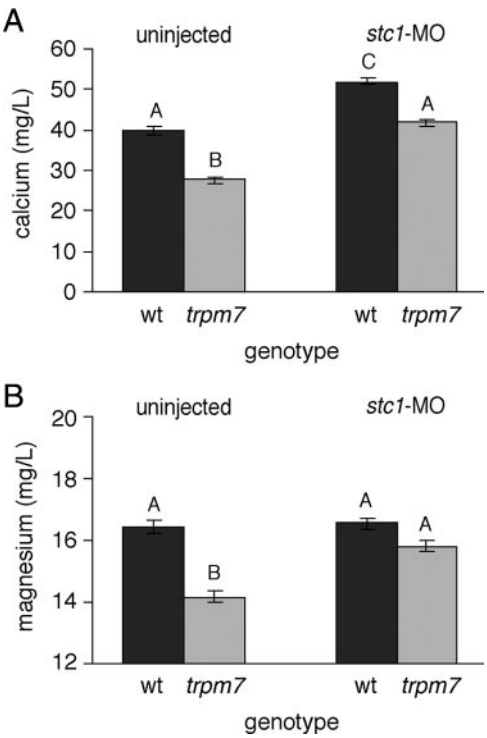

FIG. 5. Restored cation levels in *stc1* morpholino-injected larvae. A and B, *trpm7* mutant larvae injected with stc1-MO exhibit calcium (A) and magnesium (B) levels restored to wild-type (wt) levels. Furthermore, wild-type embryos injected with the stc1cs-MO exhibit significantly increased total calcium (A) as compared with uninjected wild-type siblings, although total magnesium (B) of injected and uninjected wild-type embryos did not differ significantly. By overall ANOVA, calcium $F_{(3,28)} = 29.2$ ($P < 0.0001$) and magnesium $F_{(3,28)} = 14.2$ ($P < 0.0001$). Means with the *same letters* are not significantly different from one another other within each assay using a Tukey-Kramer honestly significant difference test ($\alpha = 0.050$).

wild type (as observed also in Ref. 51). Moreover, *trpm7* mutants injected with stc1-MO exhibited total calcium and total magnesium restored to levels comparable to those of uninjected wild-type siblings (Fig. 5). As expected, wild-type siblings injected with stc1-MO showed an increase in total calcium relative to uninjected siblings (51) yet failed to exhibit altered levels of total magnesium. These results show that stc1 influences magnesium levels in the *trpm7* mutant background and that wild-type *trpm7* masks this effect. Together, these data suggest that total calcium levels are misregulated in *trpm7* mutants due to the overexpression of *stc1* and that total magnesium levels can be restored in an *stc1*-dependent, but *trpm7*-independent, manner.

An early larval defect in kidney function

In addition to effects on calcium and magnesium homeostasis demonstrated above, we showed previously that zebrafish *trpm7* mutants develop mineralized deposits in the kidneys by late larval stages (30). Because *trpm7* is expressed in the earlier pronephros as well (30, 31, 52), we asked whether *trpm7* mutants exhibit defects in kidney function as embryos or early larvae. To test this possibility, we examined early larvae for signs of kidney stone formation using the vital dye alizarin red (53, 54). We detected kidney stones in *trpm7* mutants at 5 dpf (Fig. 6A) but not at 2–4 dpf (data not shown). Kidney stones were present in 57–94% of homozygous mutants per clutch but only 0–1.4% of wild-type siblings (*trpm7*/+ and +/+; mutants *vs.* wild-type: $\chi^2 = 619$; $P < 0.0001$). Although the incidence of kidney stone formation differed significantly between families ($\chi^2 = 27.1$; $P = 0 < 0.0001$), it did not differ among mutant alleles that were lethal either at early larval stages (*trpm7*^{j124e1}, *trpm7*^{b508}) or viable (*trpm7*^{j124e2}) ($\chi^2 = 0.9$; $P = 0.6$). By repeated imaging of individual larvae, we further showed that kidney stones transit through the pronephros, demonstrating their presence in the pronephric lumen rather than in the epithelium itself (Fig. 6B).

Kidney stones in humans most often comprise deposits of calcium oxalate or calcium phosphate (55, 56), and staining of *trpm7* mutant kidney stones with alizarin red and calcein (30, 57) suggests a similar composition in zebrafish. Given the effect *stc1* on calcium homeostasis, we asked whether elevated *stc1* might be responsible for kidney stone formation in *trpm7* mutants. Contrary to this expectation, however, heat-shocked, wild-type *Tg*(*hsp70::stc1-IRES-EGFP*) embryos failed to develop kidney stones, and morpholino knockdown of *stc1* in *trpm7* mutants failed to reduce kidney stone incidence ($\chi^2 = 0.01$; $P = 0.9$).

We next considered the anti-hyperphosphatemic factor *fgf23* (58) as a candidate *trpm7*-dependent effector of kidney stone formation. Later larval skeletal defects in *trpm7* mutants are consistent with defects in both calcium and

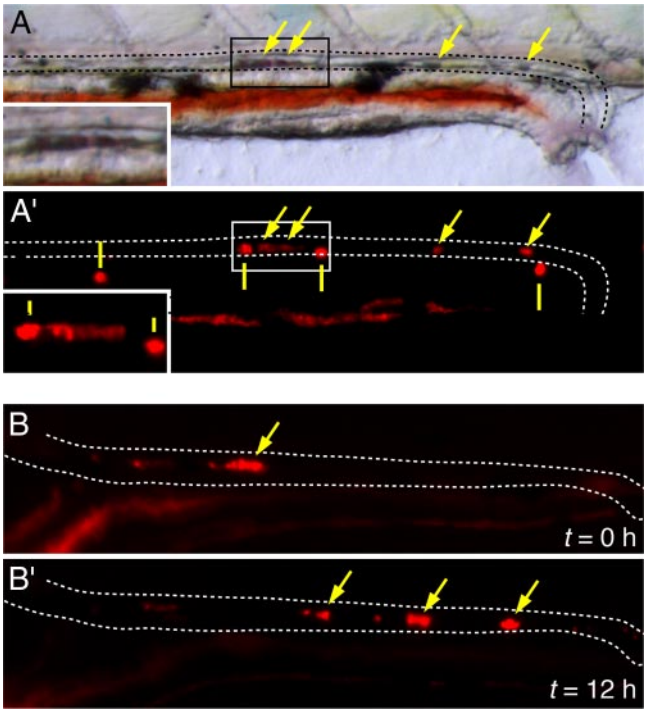

FIG. 6. Kidney stone formation and movement through pronephric duct in early-larval *trpm7* mutants. A, Bright-field (A) and fluorescent (A′) views of alizarin red-stained kidney stone in the pronephric tubule of a 5-dpf *trpm7* mutant. *Dashed lines* indicate the dorsal and ventral margins of the pronephric duct. *Arrows* indicate alizarin red-stained kidney stone visible in both bright-field and fluorescent views. *Solid vertical lines* indicate reflective pigment cells (iridophores) that are evident in epifluorescent illumination using both the mCherry filter set (shown) and EGFP filter set (not shown). *Insets*, Higher-magnification views of *boxed areas* in *main panels*. B, Kidney stones transit through the pronephric duct as revealed by repeated imaging. Shown are kidney stones that have moved through the pronephric duct lumen after 12 h after first imaging.

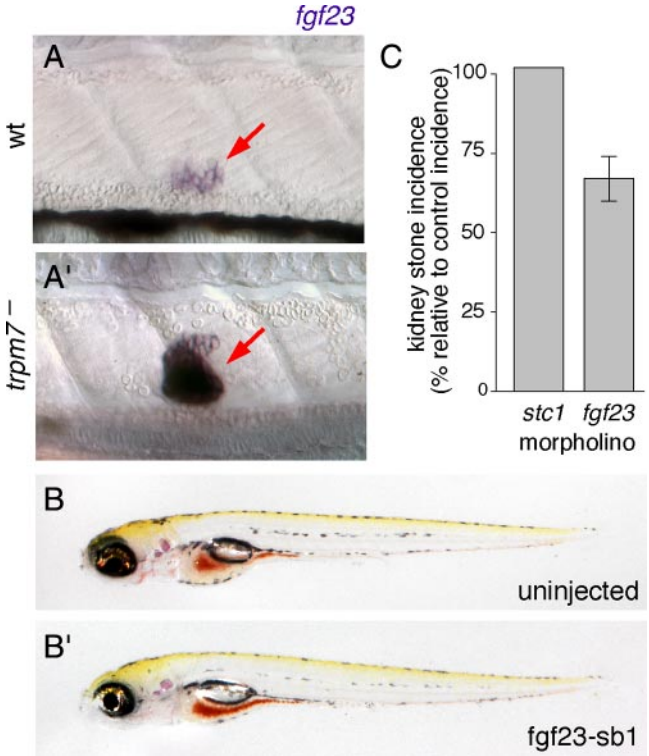

FIG. 7. *fgf23* up-regulation in *trpm7* mutants and effect of knockdown on kidney stone incidence. A, *fgf23* is weakly expressed expressed in CS (*arrow*, A) of wild-type (wt) larvae but is strongly up-regulated in *trpm7* mutant siblings (A′) at 4 dpf. (Different orientation of CS from that shown in Fig. 2B is not unusual at this stage.) B, *trpm7* mutants injected with fgf-sb1 morpholino are not morphologically distinguishable from uninjected siblings. C, *fgf23* knockdown in *trpm7* mutants reduces the incidence of kidney stones compared with uninjected controls ($\chi^2 = 11.0$; $P < 0.001$), whereas *stc1* knockdown has no effect. Values are least squares means ± SE, normalized to the incidence of kidney stones in uninjected *trpm7* mutant siblings.

phosphate homeostasis (30), and elevated fgf23 levels are associated with calcium-containing kidney stones in human patients with renal phosphate wasting and hypophosphatemia (59). We found that at 4–5 dpf, *fgf23* is expressed principally in the CS and that *trpm7* mutants exhibited a dramatic increase in transcript abundance compared with the wild type (Fig. 7A). To see whether increased *fgf23* expression might contribute to kidney stone formation, we knocked down *fgf23* using a splice-blocking morpholino, fgf23-sb1. The *trpm7* mutants injected with fgf23-sb1 were morphologically indistinguishable from uninjected controls yet exhibited a significantly reduced incidence of kidney stones (Fig. 7, B and C). Injection of wild-type embryos with fgf23-sb1 did not cause morphological defects. Finally, coinjections of *trpm7* mutants with fgf23-sb1 and stc1-MO failed to reveal synergistic interactions (data not shown). These data indicate that *trpm7* acts upstream of *fgf23* and strongly suggest that *trpm7* mutation alters not only calcium and magnesium homeostasis through *stc1* but also phosphate homeostasis through *fgf23*, with the latter contributing to kidney stone formation.

Discussion

Our study links mutation of *trpm7* to *stc1*-dependent dysregulation of calcium and magnesium homeostasis and to *fgf23*-dependent early larval kidney stone formation. We demonstrated that *trpm7* mutants exhibit reduced total calcium and reduced total magnesium at 3 and 4 dpf, respectively. By transgenic overexpression and morpholino oligonucleotide knockdown, we found that *stc1* can modulate both calcium and magnesium levels in zebrafish; up-regulated *stc1* in a wild-type background decreases total calcium and total magnesium, whereas inhibition of *stc1* translation increases these cations to wild-type levels in *trpm7* mutants. We also showed that kidney stones, previously detected in *trpm7* mutants at later larval stages (30), are evident by 5 dpf in the pronephros. Finally, we demonstrated that *trpm7* mutants overexpress *fgf23*,

whereas knockdown of *fgf23* reduces the incidence of kidney stones in the mutant background.

This study demonstrates an association between *trpm7* and physiological cation homeostasis *in vivo*. The reduced total magnesium and total calcium evident in *trpm7* mutants is similar to the hypomagnesemia and hypocalcemia resulting from *Trpm6* defects in mammals: decreased magnesium absorption likely via both intestine and kidney leads to parathyroid failure with attendant defects in calcium homeostasis leading to hypocalcemia (14, 28, 60–63). In zebrafish *trpm7* mutants, however, reduced total calcium is evident at 3 dpf, whereas reduced total magnesium is not detectable until 4 dpf. This reversal in onset raises the possibility that reduced total magnesium is secondary to reduced total calcium in *trpm7* mutants. An explanation for this difference may reside in overall differences in mammalian and teleost physiology and the relationships of these organisms with their environments as well as differences in specific molecular mediators that remain to be elucidated

Our study revealed that *trpm7* mutants exhibited higher levels of transcript for the anti-hypercalcemic factor stc1 and lower levels of calcium. Given that stanniocalcins are normally induced by high levels of serum calcium (50, 64), our data highlight the dysregulation of normal homeostatic mechanisms in the *trpm7* mutant background. These observations further raise the possibility of a direct or indirect genetic interaction by which *trpm7* regulates *stc1*. One possibility is that the kinase domain of trpm7 normally modulates the activity of Ca-sensing receptor (CaSR) within the CS. Consistent with this idea, a pharmacological activator of CaSR stimulates *stc1* expression in salmon (65), and CaSR is expressed within the CS of flounder (49). Nevertheless, our data do not exclude the possibility that *trpm7* effects on *stc1* expression may be less direct and perhaps mediated through somatic tissues other than the CS. Indeed, it is also formally possible that increased *stc1* expression in *trpm7* mutants arises secondarily to decreased calcium and magnesium levels in this genetic background. Such an effect would run counter to the typical induction of stc1 by high calcium levels and would suggest a regulatory mechanism not previously described. The generation of transgenic lines to perturb trpm7 activity in a tissue-specific manner, and further studies to identify and characterize stanniocalcin 1 receptors and interactors will likely provide important insights into these questions.

An intriguing result from our study was the restoration of total magnesium levels in *trpm7* mutants after morpholino knockdown of *stc1*. In contrast to calcium, stanniocalcin expression is not modulated by magnesium, and stanniocalcins are not known to directly influence magnesium homeostasis (64). Nevertheless, our results are concordant with a previous study, which showed that activation of CaSR led to increased levels of stc1 and decreases not only in serum calcium but in serum magnesium as well (49). The *trpm7*-independent correction of total magnesium levels we found implies a still-unknown mechanism for magnesium uptake. A potential mediator of such magnesium uptake in zebrafish would be claudin-16. In mammals, claudin-16 function in the loop of Henle is critical for passive, paracellular divalent cation reabsorption (66) and is distinct from the active, transcellular transport of magnesium by Trpm6/Trpm7 complexes. In zebrafish, we envision that claudin-16 may be regulated by *stc1* and influences the paracellular transport of both magnesium and calcium in *trpm7* mutants. The paracellular mechanism for claudin-16 transport is distinct from the transcellular mechanism of trpm6/trpm7 channels. Consequently, stc1-regulated claudin-16 activity could function as a *trpm7*-independent compensatory mechanism. Although a zebrafish ortholog of claudin-16 has not been identified, the presence of such genes in other fishes (67, 68) suggests one may yet be found.

Our study also provides insights into the development and physiological bases of kidney stone formation in *trpm7* mutants. Consistent with a defect in phosphate homeostasis, we detected strongly increased expression of *fgf23* in the CS, and we showed that knockdown of *fgf23* reduces the incidence of kidney stone development. In humans, activating mutations in *FGF23* cause autosomal dominant hypophosphatemic rickets, and tumor-produced fibroblast growth factor 23 (FGF23) results in osteomalacia (69–73), whereas mouse knockouts of *Fgf23* develop hyperphosphatemia (74, 75). Alterations in FGF23 signaling are also associated with several other pathologies including chronic kidney disease (58) and the presence of calcium-containing kidney stones in patients with hypophosphatemia and urinary phosphate wasting (59). In mammals, Fgf23 is produced primarily by bone and affects phosphate regulation by signaling through FGF receptor 1c and Klotho in the kidney (58, 76–78). Our findings suggest that CS-derived fgf23 is an early regulator of phosphate homeostasis in zebrafish, although low absolute levels of phosphate precluded the direct detection of differences in phosphate levels between wild-type and *trpm7* mutants. We speculate that kidney stone formation in the pronephric tubules may result from a localized decrease in the reabsorption of calcium, owing to reduced trpm7 channel activity, leading to increased precipitation of calcium phosphate. That fgf23 knockdown did not eliminate kidney stone formation completely may reflect limited morpholino efficacy at 5 dpf (79) or a dependence on other factors. One candidate for such an ef-

fect is *stc1*. Although we did not observe a reduction in kidney stone incidence after injecting *stc1* morpholino, either singly or in combination with *fgf23* morpholino, and *stc1* overexpression did not induce kidney stone formation in wild-type embryos, these outcomes may reflect limited perdurance of morpholinos as well as homeostatic regulation leading to resistance in the wild type that is absent or diminished in *trpm7* mutants. Indeed, *stc1* has been associated with phosphate homeostasis previously (49, 80). The isolation of *stc1* and *fgf23* mutants by targeted resequencing of mutagenized genomes or other approaches (81) would greatly facilitate the testing of homeostatic roles for these factors at stages not amenable to morpholino perturbation.

Finally, we have characterized the early-larval effects of increased *stc1* and *fgf23* on cation homeostasis and kidney stone formation, respectively, but we anticipate that both of these factors may contribute to later-stage *trpm7* mutant defects in growth and bone development as well (30). Studies of mammalian stanniocalcins and fgf23 have linked each to skeletal and growth defects (50, 72, 73, 82–86) similar to those found in *trpm7* mutants at later larval stages. Moreover, a mouse mutant for the *trpm7*-related gene transient receptor potential vanilloid 5 (*Trpv5*) exhibits urinary calcium and phosphate wasting as well as skeletal defects (87, 88), and mice doubly mutant for *Trpv5* and *CaSR* have growth retardation and develop kidney stones (89), much like zebrafish *trpm7* mutants. It will be interesting to identify the other parallels between molecular regulators of these phenotypes in teleost and mammalian models as well as in human disease.

Acknowledgments

We thank S. Pham for assistance with fish rearing and kidney stone analyses, J. Lee-Barber for analyses of morpholino effects on splicing, and two anonymous referees for helpful comments on the manuscript.

Address all correspondence and requests for reprints to: Dr. D. M. Parichy, Department of Biology, University of Washington, Box 351800, Seattle, Washington 98195. E-mail: dparichy@u.washington.edu.

This work was supported by NIH R01 HD40165 and NIH P01 GM078195. M.R.E. was funded by NRSA F31 DK074369.

Disclosure Summary: The authors have nothing to declare.

References

1. **Runnels LW, Yue L, Clapham DE** 2001 TRP-PLIK, a bifunctional protein with kinase and ion channel activities. Science 291:1043–1047
2. **Ryazanova LV, Dorovkov MV, Ansari A, Ryazanov AG** 2004 Characterization of the protein kinase activity of TRPM7/ChaK1, a protein kinase fused to the transient receptor potential ion channel. J Biol Chem 279:3708–3716
3. **Takezawa R, Schmitz C, Demeuse P, Scharenberg AM, Penner R, Fleig A** 2004 Receptor-mediated regulation of the TRPM7 channel through its endogenous protein kinase domain. Proc Natl Acad Sci USA 101:6009–6014
4. **Demeuse P, Penner R, Fleig A** 2006 TRPM7 channel is regulated by magnesium nucleotides via its kinase domain. J Gen Physiol 127: 421–434
5. **Thébault S, Cao G, Venselaar H, Xi Q, Bindels RJ, Hoenderop JG** 2008 Role of the α-kinase domain in transient receptor potential melastatin 6 channel and regulation by intracellular ATP. J Biol Chem 283:19999–20007
6. **Topala CN, Groenestege WT, Thébault S, van den Berg D, Nilius B, Hoenderop JG, Bindels RJ** 2007 Molecular determinants of permeation through the cation channel TRPM6. Cell Calcium 41:513–523
7. **Voets T, Nilius B, Hoefs S, van der Kemp AW, Droogmans G, Bindels RJ, Hoenderop JG** 2004 TRPM6 forms the Mg^{2+} influx channel involved in intestinal and renal Mg^{2+} absorption. J Biol Chem 279:19–25
8. **Li M, Du J, Jiang J, Ratzan W, Su LT, Runnels LW, Yue L** 2007 Molecular determinants of Mg^{2+} and Ca^{2+} permeability and pH sensitivity in TRPM6 and TRPM7. J Biol Chem 282:25817–25830
9. **Nadler MJ, Hermosura MC, Inabe K, Perraud AL, Zhu Q, Stokes AJ, Kurosaki T, Kinet JP, Penner R, Scharenberg AM, Fleig A** 2001 LTRPC7 is a Mg·ATP-regulated divalent cation channel required for cell viability. Nature 411:590–595
10. **Monteilh-Zoller MK, Hermosura MC, Nadler MJ, Scharenberg AM, Penner R, Fleig A** 2003 TRPM7 provides an ion channel mechanism for cellular entry of trace metal ions. J Gen Physiol 121:49–60
11. **Schmitz C, Perraud AL, Johnson CO, Inabe K, Smith MK, Penner R, Kurosaki T, Fleig A, Scharenberg AM** 2003 Regulation of vertebrate cellular Mg^{2+} homeostasis by TRPM7. Cell 114:191–200
12. **Schlingmann KP, Waldegger S, Konrad M, Chubanov V, Gudermann T** 2007 TRPM6 and TRPM7–Gatekeepers of human magnesium metabolism. Biochim Biophys Acta 1772:813–821
13. **Schmitz C, Deason F, Perraud AL** 2007 Molecular components of vertebrate Mg^{2+}-homeostasis regulation. Magnesium Research 20: 6–18
14. **Walder RY, Landau D, Meyer P, Shalev H, Tsolia M, Borochowitz Z, Boettger MB, Beck GE, Englehardt RK, Carmi R, Sheffield VC** 2002 Mutation of TRPM6 causes familial hypomagnesemia with secondary hypocalcemia. Nat Genet 31:171–174
15. **Chubanov V, Schlingmann KP, Wäring J, Heinzinger J, Kaske S, Waldegger S, Mederos y Schnitzler M, Gudermann T** 2007 Hypomagnesemia with secondary hypocalcemia due to a missense mutation in the putative pore-forming region of TRPM6. J Biol Chem 282:7656–7667
16. **Schmitz C, Dorovkov MV, Zhao X, Davenport BJ, Ryazanov AG, Perraud AL** 2005 The channel kinases TRPM6 and TRPM7 are functionally nonredundant. J Biol Chem 280:37763–37771
17. **Li M, Jiang J, Yue L** 2006 Functional characterization of homo- and heteromeric channel kinases TRPM6 and TRPM7. J Gen Physiol 127:525–537
18. **Fujiwara Y, Minor Jr DL** 2008 X-ray crystal structure of a TRPM assembly domain reveals an antiparallel four-stranded coiled-coil. J Mol Biol 383:854–870
19. **Chubanov V, Waldegger S, Mederos y Schnitzler M, Vitzthum H, Sassen MC, Seyberth HW, Konrad M, Gudermann T** 2004 Disruption of TRPM6/TRPM7 complex formation by a mutation in the TRPM6 gene causes hypomagnesemia with secondary hypocalcemia. Proc Natl Acad Sci USA 101:2894–2899
20. **Fonfria E, Murdock PR, Cusdin FS, Benham CD, Kelsell RE, McNulty S** 2006 Tissue distribution profiles of the human TRPM cation channel family. J Recept Signal Transduct Res 26:159–178
21. **Groenestege WM, Hoenderop JG, van den Heuvel L, Knoers N, Bindels RJ** 2006 The epithelial Mg^{2+} channel transient receptor

potential melastatin 6 is regulated by dietary Mg^{2+} content and estrogens. J Am Soc Nephrol 17:1035–1043
22. **Kunert-Keil C, Bisping F, Krüger J, Brinkmeier H** 2006 Tissue-specific expression of TRP channel genes in the mouse and its variation in three different mouse strains. BMC Genomics 7:159
23. **Krapivinsky G, Mochida S, Krapivinsky L, Cibulsky SM, Clapham DE** 2006 The TRPM7 ion channel functions in cholinergic synaptic vesicles and affects transmitter release. Neuron 52:485–496
24. **Wei WL, Sun HS, Olah ME, Sun X, Czerwinska E, Czerwinski W, Mori Y, Orser BA, Xiong ZG, Jackson MF, Tymianski M, MacDonald JF** 2007 TRPM7 channels in hippocampal neurons detect levels of extracellular divalent cations. Proc Natl Acad Sci USA 104:16323–16328
25. **Aarts M, Iihara K, Wei WL, Xiong ZG, Arundine M, Cerwinski W, MacDonald JF, Tymianski M** 2003 A key role for TRPM7 channels in anoxic neuronal death. Cell 115:863–877
26. **Su LT, Agapito MA, Li M, Simonson WT, Huttenlocher A, Habas R, Yue L, Runnels LW** 2006 TRPM7 regulates cell adhesion by controlling the calcium-dependent protease calpain. J Biol Chem 281:11260–11270
27. **Clark K, Langeslag M, van Leeuwen B, Ran L, Ryazanov AG, Figdor CG, Moolenaar WH, Jalink K, van Leeuwen FN** 2006 TRPM7, a novel regulator of actomyosin contractility and cell adhesion. EMBO J 25:290–301
28. **Schlingmann KP, Weber S, Peters M, Niemann Nejsum L, Vitzthum H, Klingel K, Kratz M, Haddad E, Ristoff E, Dinour D, Syrrou M, Nielsen S, Sassen M, Waldegger S, Seyberth HW, Konrad M** 2002 Hypomagnesemia with secondary hypocalcemia is caused by mutations in TRPM6, a new member of the TRPM gene family. Nat Genet 31:166–170
29. **Jin J, Desai BN, Navarro B, Donovan A, Andrews NC, Clapham DE** 2008 Deletion of Trpm7 disrupts embryonic development and thymopoiesis without altering Mg^{2+} homeostasis. Science 322:756–760
30. **Elizondo MR, Arduini BL, Paulsen J, MacDonald EL, Sabel JL, Henion PD, Cornell RA, Parichy DM** 2005 Defective skeletogenesis with kidney stone formation in dwarf zebrafish mutant for trpm7. Curr Biol 15:667–671
31. **Thisse B, Heyer V, Lux A, Alunni V, Seiliez I, Kirchner J, Parkhill J-P, Thisse C** 2004 Spatial and temporal expression of the zebrafish genome by large-scale in situ hybridization screening. Methods Cell Biol 77:505–551
32. **Krishnamurthy VG** 1976 Cytophysiology of corpuscles of Stannius. Int Rev Cytol 46:177–249
33. **McNeill MS, Paulsen J, Bonde G, Burnight E, Hsu MY, Cornell RA** 2007 Cell death of melanophores in zebrafish trpm7 mutant embryos depends on melanin synthesis. J Invest Dermatol 127:2020–2030
34. **Arduini BL, Henion PD** 2004 Melanophore sublineage-specific requirement for zebrafish touchtone during neural crest development. Mech Dev 121:1353–1364
35. **Cornell RA, Yemm E, Bonde G, Li W, d'Alençon C, Wegman L, Eisen J, Zahs A** 2004 Touchtone promotes survival of embryonic melanophores in zebrafish. Mech Dev 121:1365–1376
36. **Pfaffl MW, Horgan GW, Dempfle L** 2002 Relative expression software tool (REST) for group-wise comparison and statistical analysis of relative expression results in real-time PCR. Nucleic Acids Res 30:e36
37. **Simon P** 2003 Q-Gene: processing quantitative real-time RT-PCR data. Bioinformatics 19:1439–1440
38. **Thisse C, Thisse B** 2008 High-resolution in situ hybridization to whole-mount zebrafish embryos. Nat Protoc 3:59–69
39. **Corey DP, Garcia-Anoveros J, Holt JR, Kwan KY, Lin SY, Vollrath MA, Amalfitano A, Cheung EL, Derfler BH, Duggan A, Geleoc GS, Gray PA, Hoffman MP, Rehm HL, Tamasauskas D, Zhang DS** 2004 TRPA1 is a candidate for the mechanosensitive transduction channel of vertebrate hair cells. Nature 432:723–730
40. **Kwan KM, Fujimoto E, Grabher C, Mangum BD, Hardy ME, Campbell DS, Parant JM, Yost HJ, Kanki JP, Chien CB** 2007 The Tol2kit: a multisite gateway-based construction kit for Tol2 transposon transgenesis constructs. Dev Dyn 236:3088–3099
41. **Draper BW, Morcos PA, Kimmel CB** 2001 Inhibition of zebrafish fgf8 pre-mRNA splicing with morpholino oligos: a quantifiable method for gene knockdown. Genesis 30:154–156
42. **Westerfield M** 2000 The zebrafish book. A guide for the laboratory use of zebrafish (*Danio rerio*). 4th ed. Eugene, Oregon: University of Oregon Press
43. **Akerström G, Hellman P, Hessman O, Segersten U, Westin G** 2005 Parathyroid glands in calcium regulation and human disease. Ann NY Acad Sci 1040:53–58
44. **Rankin W, Grill V, Martin TJ** 1997 Parathyroid hormone-related protein and hypercalcemia. Cancer 80:1564–1571
45. **Talmage RV, Mobley HT** 2008 Calcium homeostasis: reassessment of the actions of parathyroid hormone. Gen Comp Endocrinol 156:1–8
46. **Pandey AC** 1994 Evidence for general hypocalcemic hormone from the stannius corpuscles of the freshwater catfish Ompok bimaculatus (Bl). Gen Comp Endocrinol 94:182–185
47. **Lafeber FP, Flik G, Wendelaar Bonga SE, Perry SF** 1988 Hypocalcin from Stannius corpuscles inhibits gill calcium uptake in trout. Am J Physiol 254:R891–R896
48. **Sundell K, Björnsson BT, Itoh H, Kawauchi H** 1992 Chum salmon (*Oncorhynchus keta*) stanniocalcin inhibits in vitro intestinal calcium uptake in Atlantic cod (*Gadus morhua*). J Comp Physiol B 162:489–495
49. **Greenwood MP, Flik G, Wagner GF, Balment RJ** 2009 The corpuscles of Stannius, calcium-sensing receptor, and stanniocalcin: responses to calcimimetics and physiological challenges. Endocrinology 150:3002–3010
50. **Wagner GF, Dimattia GE** 2006 The stanniocalcin family of proteins. J Exp Zool A Comp Exp Biol 305:769–780
51. **Tseng DY, Chou MY, Tseng YC, Hsiao CD, Huang CJ, Kaneko T, Hwang PP** 2009 Effects of stanniocalcin 1 on calcium uptake in zebrafish (Danio rerio) embryo. Am J Physiol Regul Integr Comp Physiol 296:R549–R557
52. **Wingert RA, Selleck R, Yu J, Song HD, Chen Z, Song A, Zhou Y, Thisse B, Thisse C, McMahon AP, Davidson AJ** 2007 The cdx genes and retinoic acid control the positioning and segmentation of the zebrafish pronephros. PLoS Genet 3:1922–1938
53. **Nemoto Y** 2007 Calcein and alizarin complexone staining In: Wakamatsu Y, ed. Medaka book: a guide for the laboratory use of medaka (*Oryzias latipes*). Nagoya, Japan: Nagoya University
54. **Walker MB, Kimmel CB** 2007 A two-color acid-free cartilage and bone stain for zebrafish larvae. Biotech Histochem 82:23–28
55. **Evan AP** 2010 Physiopathology and etiology of stone formation in the kidney and the urinary tract. Pediatr Nephrol 25:831–841
56. **Moe OW** 2006 Kidney stones: pathophysiology and medical management. Lancet 367:333–344
57. **Du SJ, Frenkel V, Kindschi G, Zohar Y** 2001 Visualizing normal and defective bone development in zebrafish embryos using the fluorescent chromophore calcein. Dev Biol 238:239–246
58. **Marsell R, Jonsson KB** 5 July 2010 The phosphate regulating hormone FGF23. Acta Physiol (Oxf) 10.1111/j.1748-1716.2010.02163.x
59. **Rendina D, Mossetti G, De Filippo G, Cioffi M, Strazzullo P** 2006 Fibroblast growth factor 23 is increased in calcium nephrolithiasis with hypophosphatemia and renal phosphate leak. J Clin Endocrinol Metab 91:959–963
60. **Yamamoto T, Kabata H, Yagi R, Takashima M, Itokawa Y** 1985 Primary hypomagnesemia with secondary hypocalcemia. Report of a case and review of the world literature. Magnesium 4:153–164
61. **Milla PJ, Aggett PJ, Wolff OH, Harries JT** 1979 Studies in primary hypomagnesaemia: evidence for defective carrier-mediated small intestinal transport of magnesium. Gut 20:1028–1033
62. **Knoers NV** 2009 Inherited forms of renal hypomagnesemia: an update. Pediatr Nephrol 24:697–705

63. **Anast CS, Mohs JM, Kaplan SL, Burns TW** 1972 Evidence for parathyroid failure in magnesium deficiency. Science 177:606–608
64. **Wagner GF, Jaworski E** 1994 Calcium regulates stanniocalcin mRNA levels in primary cultured rainbow trout corpuscles of stannius. Mol Cell Endocrinol 99:315–322
65. **Radman DP, McCudden C, James K, Nemeth EM, Wagner GF** 2002 Evidence for calcium-sensing receptor mediated stanniocalcin secretion in fish. Mol Cell Endocrinol 186:111–119
66. **Kausalya PJ, Amasheh S, Günzel D, Wurps H, Müller D, Fromm M, Hunziker W** 2006 Disease-associated mutations affect intracellular traffic and paracellular Mg^{2+} transport function of Claudin-16. J Clin Invest 116:878–891
67. **Kollmar R, Nakamura SK, Kappler JA, Hudspeth AJ** 2001 Expression and phylogeny of claudins in vertebrate primordia. Proc Natl Acad Sci USA 98:10196–10201
68. **Loh YH, Christoffels A, Brenner S, Hunziker W, Venkatesh B** 2004 Extensive expansion of the claudin gene family in the teleost fish, Fugu rubripes. Genome Res 14:1248–1257
69. **Shimada T, Yamazaki Y, Takahashi M, Hasegawa H, Urakawa I, Oshima T, Ono K, Kakitani M, Tomizuka K, Fujita T, Fukumoto S, Yamashita T** 2005 Vitamin D receptor-independent FGF23 actions in regulating phosphate and vitamin D metabolism. Am J Physiol Renal Physiol 289:F1088–F1095
70. **White KE, Carn G, Lorenz-Depiereux B, Benet-Pages A, Strom TM, Econs MJ** 2001 Autosomal-dominant hypophosphatemic rickets (ADHR) mutations stabilize FGF-23. Kidney Int 60:2079–2086
71. **White KE, Jonsson KB, Carn G, Hampson G, Spector TD, Mannstadt M, Lorenz-Depiereux B, Miyauchi A, Yang IM, Ljunggren O, Meitinger T, Strom TM, Jüppner H, Econs MJ** 2001 The autosomal dominant hypophosphatemic rickets (ADHR) gene is a secreted polypeptide overexpressed by tumors that cause phosphate wasting. J Clin Endocrinol Metab 86:497–500
72. **Jonsson KB, Zahradnik R, Larsson T, White KE, Sugimoto T, Imanishi Y, Yamamoto T, Hampson G, Koshiyama H, Ljunggren O, Oba K, Yang IM, Miyauchi A, Econs MJ, Lavigne J, Jüppner H** 2003 Fibroblast growth factor 23 in oncogenic osteomalacia and X-linked hypophosphatemia. N Engl J Med 348:1656–1663
73. **ADHR-Consortium** 2000 Autosomal dominant hypophosphataemic rickets is associated with mutations in FGF23. Nat Genet 26: 345–348
74. **Sitara D, Razzaque MS, Hesse M, Yoganathan S, Taguchi T, Erben RG, Jüppner H, Lanske B** 2004 Homozygous ablation of fibroblast growth factor-23 results in hyperphosphatemia and impaired skeletogenesis, and reverses hypophosphatemia in Phex-deficient mice. Matrix Biol 23:421–432
75. **Shimada T, Kakitani M, Yamazaki Y, Hasegawa H, Takeuchi Y, Fujita T, Fukumoto S, Tomizuka K, Yamashita T** 2004 Targeted ablation of Fgf23 demonstrates an essential physiological role of FGF23 in phosphate and vitamin D metabolism. J Clin Invest 113: 561–568
76. **Farrow EG, Davis SI, Summers LJ, White KE** 2009 Initial FGF23-mediated signaling occurs in the distal convoluted tubule. J Am Soc Nephrol 20:955–960
77. **Goetz R, Nakada Y, Hu MC, Kurosu H, Wang L, Nakatani T, Shi M, Eliseenkova AV, Razzaque MS, Moe OW, Kuro-o M, Mohammadi M** 2010 Isolated C-terminal tail of FGF23 alleviates hypophosphatemia by inhibiting FGF23-FGFR-Klotho complex formation. Proc Natl Acad Sci USA 107:407–412
78. **Urakawa I, Yamazaki Y, Shimada T, Iijima K, Hasegawa H, Okawa K, Fujita T, Fukumoto S, Yamashita T** 2006 Klotho converts canonical FGF receptor into a specific receptor for FGF23. Nature 444:770–774
79. **Nasevicius A, Ekker SC** 2000 Effective targeted gene 'knockdown' in zebrafish. Nat Genet 26:216–220
80. **Lu M, Wagner GF, Renfro JL** 1994 Stanniocalcin stimulates phosphate reabsorption by flounder renal proximal tubule in primary culture. Am J Physiol 267:R1356–R1362
81. **Skromne I, Prince VE** 2008 Current perspectives in zebrafish reverse genetics: moving forward. Dev Dyn 237:861–882
82. **Varghese R, Gagliardi AD, Bialek PE, Yee SP, Wagner GF, Dimattia GE** 2002 Overexpression of human stanniocalcin affects growth and reproduction in transgenic mice. Endocrinology 143:868–876
83. **Wu S, Yoshiko Y, De Luca F** 2006 Stanniocalcin 1 acts as a paracrine regulator of growth plate chondrogenesis. J Biol Chem 281:5120–5127
84. **Filvaroff EH, Guillet S, Zlot C, Bao M, Ingle G, Steinmetz H, Hoeffel J, Bunting S, Ross J, Carano RA, Powell-Braxton L, Wagner GF, Eckert R, Gerritsen ME, French DM** 2002 Stanniocalcin 1 alters muscle and bone structure and function in transgenic mice. Endocrinology 143:3681–3690
85. **Gagliardi AD, Kuo EY, Raulic S, Wagner GF, DiMattia GE** 2005 Human stanniocalcin-2 exhibits potent growth-suppressive properties in transgenic mice independently of growth hormone and IGFs. Am J Physiol Endocrinol Metab 288:E92–E105
86. **Chang AC, Hook J, Lemckert FA, McDonald MM, Nguyen MA, Hardeman EC, Little DG, Gunning PW, Reddel RR** 2008 The murine stanniocalcin 2 gene is a negative regulator of postnatal growth. Endocrinology 149:2403–2410
87. **Hoenderop JG, van Leeuwen JP, van der Eerden BC, Kersten FF, van der Kemp AW, Mérillat AM, Waarsing JH, Rossier BC, Vallon V, Hummler E, Bindels RJ** 2003 Renal Ca^{2+} wasting, hyperabsorption, and reduced bone thickness in mice lacking TRPV5. J Clin Invest 112:1906–1914
88. **Renkema KY, Nijenhuis T, van der Eerden BC, van der Kemp AW, Weinans H, van Leeuwen JP, Bindels RJ, Hoenderop JG** 2005 Hypervitaminosis D mediates compensatory Ca^{2+} hyperabsorption in TRPV5 knockout mice. J Am Soc Nephrol 16:3188–3195
89. **Renkema KY, Velic A, Dijkman HB, Verkaart S, van der Kemp AW, Nowik M, Timmermans K, Doucet A, Wagner CA, Bindels RJ, Hoenderop JG** 2009 The calcium-sensing receptor promotes urinary acidification to prevent nephrolithiasis. J Am Soc Nephrol 20:1705–1713